IEEE Access
Multidisciplinary | Rapid Review | Open Access Journal

Received October 27, 2020, accepted November 8, 2020, date of publication November 16, 2020, date of current version December 2, 2020.

Digital Object Identifier 10.1109/ACCESS.2020.3038190

Two-Step Thresholds TBD Algorithm for Time Sensitive Target Based on Dynamic Programming

YU LI, CAIPIN LI, MIN TIAN, WEIWEI WANG, CHONGDI DUAN, AND XUYAN WANG
Xi'an Institute of Space Radio Technology, Xi'an 710000, China

Corresponding author: Min Tian (458497658@qq.com)

This work was supported in part by the National Equipment Development Foundation of China under Grant 61404160108, and in part by the National Natural Science Foundation of China under Grant 61701395.

ABSTRACT Surveillance radar is confronted with serious two-dimensional ambiguity (i.e., range dimension and velocity dimension) and low signal-to-noise ratio (SNR) problems in the time sensitive (TS) target detection process, which may result in the deterioration of target detection performance. Combining the advantages of the intra-frame detection and the inter-frame detection, a novel two-step thresholds track before detect (TBD) algorithm based on the integration techniques, i.e., two-dimensional ambiguity resolution and multi-frame joint detection, is proposed in this paper. Firstly, the fusion design strategy, including the pulse repetition frequency, the carrier frequency and the orthogonal waveform, is adopted in the transmitting pulse sequence. As a result, not only the range ambiguity number and the spatial filling time are reduced synchronously, but the decoupling of range-velocity ambiguity is realized, which is conductive to multi-target detection in low SNR environment. Then, the first level adaptive threshold is obtained by employing the judgment criterion based on cumulative value function (CVF), and thus the false trajectory number is effectively eliminated from the perspective of cumulative amplitude. Finally, through analyzing the inherent relation between the local trajectory characteristics and the global trajectory characteristics comprehensively, different types of false alarm trajectories are further reduced by means of the polynomial coefficient variance statistics. Experimental results verify the effectiveness of the proposed algorithm.

INDEX TERMS Pulse sequence, track before detect, two-dimensional ambiguity, cumulative value function, trajectory characteristics.

I. INTRODUCTION

Due to the super-high speed as well as the small radar cross section (RCS) of TS targets [1], serious two-dimensional ambiguity [2], [3] and low SNR [4] problems cannot be neglected in the detection process for surveillance radar systems. TBD [5], [6] algorithms improve the target SNR based on long-term energy accumulation strategy, which is suitable for detecting weak target with small RCS. However, the multi-frame temporal-spatial correlation is destroyed as a result of the serious two-dimensional ambiguity, which makes it difficult to extract the real target trajectories.

To address the aforementioned issues, many relevant solutions from different perspectives have been presented in recent years. MMPHDF-DA algorithm [7], in which the range ambiguity is fused with the trajectory association procedure, is consolidated as the probability hypothesis density filter (PHDF) method and can realize multi-target detection by employing the mixed filtering model. Trajectory extraction approach [8] is developed by means of the multiple pulse repetition frequency (PRF) to estimate the range ambiguity number, and thus, the multi-frame trajectories are formed based on Hough transform. For high-resolution radar, weak target particle filter algorithm [9] based on the measurement model of intensity diffusion function is proposed to verify the reliability of range ambiguity resolution in the high PRF situation. In literature [10], the well-known multi-hypothesis TBD value function under the range ambiguous condition is demonstrated through constructing the extended ambiguous measurement set. However, the above algorithms

The associate editor coordinating the review of this manuscript and approving it for publication was Yu-Huei Cheng.

only give consideration to one-dimensional ambiguity case. Also, the false alarm performance has not been qualitatively evaluated.

For the false alarm trajectory elimination problem, it is difficult to completely suppress different types of trajectories via constant false alarm rate (CFAR) methods because the mixed trajectories, such as the mixed trajectories composed of noises and targets, are similar to the target trajectories in terms of the value function [11]. Another type of typical methods also referred as the trajectory characteristic approaches [12], are considered as an efficient way to further reduce the false alarm trajectory number. Trajectory overlapping algorithm [13], in the trajectory backtracking process, could eliminate the false alarm trajectories induced by target energy diffusion according to their multi-frame coincidence feature with the real target trajectory. Note that the multi-frame echoes of the noise trajectory are always irrelevant, Li method [14] based on the deviation angle statistics could eliminate this type of false alarm trajectories effectively. However, in the aforementioned algorithms, the relationship between the local trajectory characteristics and the global trajectory characteristics is not adequately exploited, and hence results in the false alarm performance degradation.

In this paper, a novel dynamic programming-track before detect (DP-TBD) algorithm based on the extended two-dimensional ambiguous measurement model is proposed, where the basic idea is that the intra-frame detection and the inter-frame detection are combined to obtain the trajectory set as well as the corresponding two-dimensional ambiguous number. Compared with the recent work, the proposed algorithm takes the inherent characteristics of TS targets into account in the two-step thresholds detection process and thus to achieve a significant detection performance improvement, which is verified from the experimental results.

The rest of this paper is organized as follows. The fundamental of the extended two-dimensional ambiguous measurement model is introduced in Section II. In Section III, the proposed two-step thresholds DP-TBD algorithm is depicted in detail, where the multi-target detection performance and the multi-frame false alarm problem are analyzed. Numerical results are given in Section IV to verify the effectiveness of the proposed method. Finally, a brief conclusion is drawn in Section V.

II. EXTENDED TWO-DIMENSIONAL AMBIGUOUS MEASUREMENT MODEL

Suppose that there are M targets in the observation scene. Radar echo is composed of K frames, each with an interval of N coherent processing intervals (CPIs), CPI_n stands for the n th coherent processing interval (CPI) during one frame. In rectangular coordinate system, the m th target motion state in CPI_n can be expressed as

$$\boldsymbol{x}_k^{m,n} = [p_{x,k}^{m,n}, v_{x,k}^{m,n}, p_{y,k}^{m,n}, v_{y,k}^{m,n}]^T \tag{1}$$

where $m = 1, 2, \cdots, M, k = 1, 2, \cdots, K, n = 1, 2, \cdots, N$, $p_{x,k}^{m,n}, p_{y,k}^{m,n}, v_{x,k}^{m,n}$ and $v_{y,k}^{m,n}$ represent the positions and velocities along X-axis and Y-axis, respectively. Thus, multi-target motion equation is given by

$$\boldsymbol{x}_k^{m,n} = \boldsymbol{F}\boldsymbol{x}_{k-1}^{m,n} \tag{2}$$

Here, the transition matrix [12] of the target motion state is represented by

$$\boldsymbol{F} = \begin{bmatrix} 1 & \sum_{i=1}^{N} CPI_n & 0 & 0 \\ 0 & 1 & 0 & 0 \\ 0 & 0 & 1 & \sum_{i=1}^{N} CPI_n \\ 0 & 0 & 0 & 1 \end{bmatrix} \tag{3}$$

For the pulse-Doppler radar, let variables $r_k^{m,n}$, $\theta_k^{m,n}$ and $v_k^{m,n}$ be the range, the azimuth angle and the radial velocity of the m th target in CPI_n, and thus the relationship with the two-dimensional positions in rectangular coordinate system is formulated as

$$\begin{cases} r_k^{m,n} = \sqrt{(p_{x,k}^{m,n})^2 + (p_{y,k}^{m,n})^2} \\ \theta_k^{m,n} = \arctan(p_{y,k}^{m,n} / p_{x,k}^{m,n}) \\ v_k^{m,n} = \sqrt{(v_{x,k}^{m,n})^2 + (v_{y,k}^{m,n})^2}\cos(\tilde{\theta}_k^{m,n}) \end{cases} \tag{4}$$

where arctan and cos denote the inverse tangent operation and the cosine operation, $\tilde{\theta}_k^{m,n}$ is the included angle of the m th target relative to the antenna's main lobe direction.

In terms of the two-dimensional ambiguity situation, the extended ambiguous range-velocity measurement model can be represented as

$$\begin{cases} \tilde{r}_k^{m,n} = r_k^{m,n} \bmod (R_w^{m,n}) + (l-1)R_w^{m,n}, \\ \qquad l = 1, 2 \cdots, R_{amb\_num}^{m,n} \\ \tilde{v}_k^{m,n} = v_k^{m,n} \bmod (v_w^{m,n}) + (s-1)v_w^{m,n}, \\ \qquad s = 1, 2 \cdots, v_{amb\_num}^{m,n} \end{cases} \tag{5}$$

where $R_w^{m,n}$ and $v_w^{m,n}$ are the maximum unambiguous range and the maximum unambiguous velocity, $R_{amb\_num}^{m,n}$ and $v_{amb\_num}^{m,n}$ are the corresponding ambiguous number in turn. $r_k^{m,n} \bmod (R_u^{m,n})$ and $v_k^{m,n} \bmod (v_u^{m,n})$ stand for the measured range and the measured velocity of the radar system.

The K frame trajectory set of M targets in the observation scene can be described as

$$\boldsymbol{X}_{1:K} = \begin{Bmatrix} (\boldsymbol{x}_{1:K}^{1,1}, & \boldsymbol{x}_{1:K}^{1,2}, & \cdots, & \boldsymbol{x}_{1:K}^{1,n}, & \cdots, & \boldsymbol{x}_{1:K}^{1,N}) \\ (\boldsymbol{x}_{1:K}^{2,1}, & \boldsymbol{x}_{1:K}^{2,2}, & \cdots, & \boldsymbol{x}_{1:K}^{2,n}, & \cdots, & \boldsymbol{x}_{1:K}^{2,N}) \\ & & \vdots & & & \\ (\boldsymbol{x}_{1:K}^{m,1}, & \boldsymbol{x}_{1:K}^{m,2}, & \cdots, & \boldsymbol{x}_{1:K}^{m,n}, & \cdots, & \boldsymbol{x}_{1:K}^{m,N}) \\ (\boldsymbol{x}_{1:K}^{M,1}, & \boldsymbol{x}_{1:K}^{M,2}, & \cdots, & \boldsymbol{x}_{1:K}^{M,n}, & \cdots, & \boldsymbol{x}_{1:K}^{M,N}) \end{Bmatrix} \tag{6}$$

According to the aforementioned ambiguous measurement model, the decision criterion of DP-TBD algorithm can be summarized as

$$\begin{cases} \boldsymbol{X}_{1:K} = \arg\max_{X_{1:T}} \boldsymbol{I}(\boldsymbol{X}_{1:K}|\boldsymbol{Z}_{1:K}) \\ s.t. \boldsymbol{I}(\boldsymbol{X}_{1:K}|\boldsymbol{Z}_{1:K}) > Threshold \end{cases} \tag{7}$$

where $s.t.$ denotes the constraint function, arg max means seeking the parameter relative to the maximum function value. *Threshold* is the multi-frame accumulation threshold, $\boldsymbol{Z}_{1:K}$ is the multi-frame measurement echo set. $\boldsymbol{I}$ represents the CVF under the two-dimensional ambiguity condition, and its construction strategy will be discussed in section III.

III. PROPOSED METHOD

A. TRANSMITTING PULSE SEQUENCE DESIGN

For the transmitting pulse sequence design, we mainly pay attention to the problem of the two-dimensional ambiguity and the spatial filling time [15]. Hence, the pulse repetition frequency, the carrier frequency and the orthogonal waveform are merged together in the subsequent process. Suppose that the cumulative pulse number during CPI_n is T_n, and the corresponding orthogonal signals can be expressed as $S_n(t)$, $t = 1, 2 \cdots, T_n$, which meet the orthogonality mutually, namely,

$$\begin{cases} S_n(t) = S_n(t + Num)(1 \le t \le T_n - Num) \\ \int S_n(t) S_n^*(t + t_0) dt = 0(1 \le t_0 \le Num - 1) \\ \int S_u(t_u) S_v^*(T_v - t_v) dt = 0(t_u, t_v \in \{1, 2\}, \\ \qquad u - \mathrm{mod}(v, N) = 1) \end{cases} \tag{8}$$

where $1 \le u, v \le N$, $(\cdot)^*$ and mod denote the conjugate operation and the remainder operation, respectively.

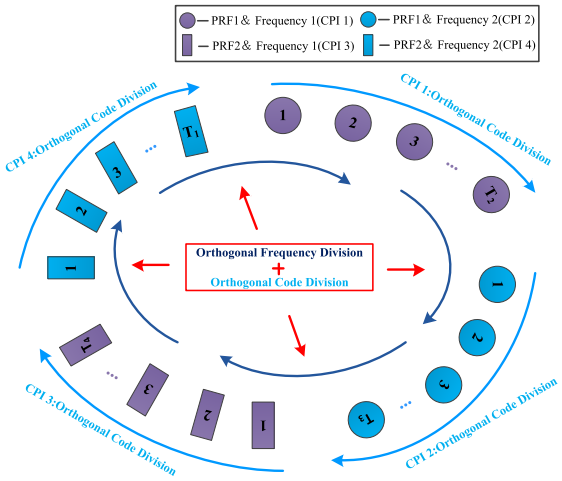

FIGURE 1. TT pulse sequence.

In this paper, through the intra-CPI orthogonal code division design as well as the inter-CPI orthogonal code division + orthogonal frequency division design, the Two PRFs & Two carrier frequencies (TT) orthogonal signal sets are adopted in the transmitting pulse sequence, where four CPI data are included in each frame, as illustrated in FIGURE. 1. This approach ensures the orthogonality for adjacent pulses, also, it is feasible for the project implementation. The transmitting pulse parameters of the four CPIs in one frame are set to (PRF_1, f_1) , (PRF_1, f_2) , (PRF_2, f_1) and (PRF_2, f_2), where PRF_1, PRF_2, f_1 and f_2 denote the two PRFs and the two carrier frequencies in the above TT pulse sequence, f_1 and f_2 satisfy $|f_2 - f_1| > B$, B is the signal bandwidth.

Compared to the typical coincidence method [16], the TT method has the following advantages.

1) Different carrier frequencies are employed in the adjacent CPIs and hence to separate different CPI data by virtue of the filters with different center frequencies, which effectively alleviate the cumulative signal-to-noise ratio (SNR) loss induced by the spatial filling time.

2) For the sake of reducing the false alarm trajectory number caused by extended two-dimensional ambiguous data, the two-dimensional ambiguity decoupling is realized using the TT pulse sequence. That is, the CPI data sets which possess the same PRF but at different carrier frequencies are firstly applied to the velocity ambiguity resolution. Then, the CPI data sets with different PRFs are employed to resolve the range ambiguity.

3) According to the aforementioned orthogonal signal model in equation (8), the range ambiguity number can be reduced to $\frac{1}{Num}$ degree.

For the TT method, it should be noted that the return data in the Doppler domain need to be converted to the velocity domain. In this way, with regard to the same target, the velocity positions related to different CPI data sets are coincident in the absence of the measurement error, and thus the coincidence method is applicable to the velocity ambiguity resolution.

B. FIRST LEVEL THRESHOLD SETTING METHOD BASED ON THE CUMULATIVE VALUE FUNCTION

For trajectory processing, considering that the accumulation amplitude formed by targets and strong noises is close to that totally formed by the real target in the trajectory backtracking process, so it is difficult for the constant false alarm (CFAR) algorithms to remove the mixed false alarm trajectories. Clearly, CFAR criterion is only applicable to eliminate the false alarm trajectories completely composed of the noise, which possesses relatively low accumulation amplitude.

In order to improve the rationality of the first level threshold, it is necessary to deeply mine the relationship between the CVF and the N independent value functions. Hence, both the two-dimensional ambiguity resolution efficiency and the multi-frame detection performance are taken into consideration through judging the trajectory composition of CVF. Here, there are two ways to generate the CVF, as depicted in FIGURE. 2. For the first generation mode of CVF, the ambiguity resolution process based on N CPI data during one frame is carried out before superposing these unambiguous data, and the CVF is achieved by associating the multi-frame data. For the second generation mode of CVF, however, the N independent value functions and the corresponding trajectories are obtained before implementing the trajectory ambiguity resolution process. On this basis, the CVF is generated based on the summation of the

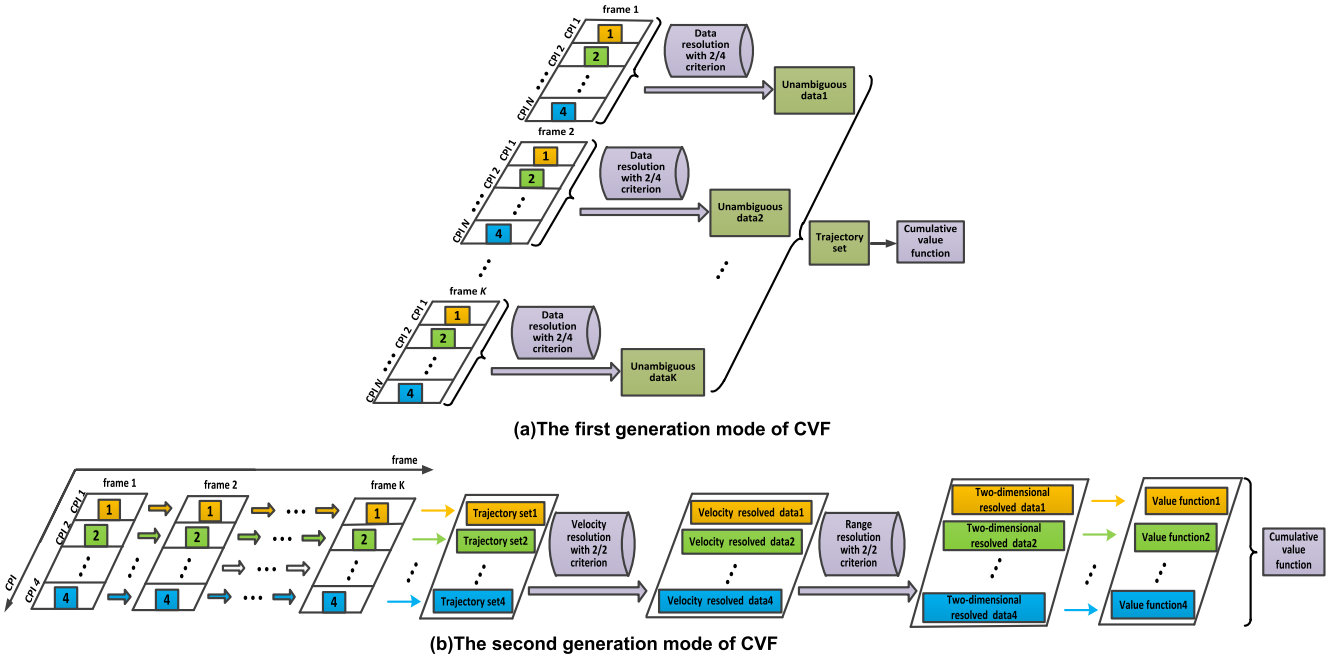

FIGURE 2. Different generation modes of CVF.

independent value functions. The advantage of the former one is that the two-dimensional ambiguity resolution is completed during one frame, which reduces the multi-frame association complexity caused by extended two-dimensional ambiguous data. However, a large number of ghost targets, especially in the serious two-dimensional ambiguity and low SNR situation, are generated when conducting the intra-frame ambiguity resolution based on the coincidence method, which greatly increase the false alarm trajectories in the trajectory backtracking process. While the advantage of the latter one lies in the generation mode of its value function, which is formed by the multi-frame trajectory data with the same CPI parameters rather than the single frame data with different CPI parameters. In this way, the false alarm issue could be mitigated by utilizing the multi-frame correlation characteristics. Also, the false alarm trajectory number can be further eliminated based on the trajectory ambiguity resolution for velocity dimension and range dimension in turn. In respect of the above CVFs, the coincidence method under M_0/N_0 criterion [17] is employed to resolve the two-dimensional ambiguity, where the definition of the data coincidence in the intra-frame ambiguity resolution process is that the measured data of different CPIs in range-velocity domain is located in the same resolution cell, and that of the trajectory coincidence in the trajectory ambiguity resolution process indicates that the measured data of different CPI within each frame is located in the same resolution cell. Here, 2/4 criterion is adopted for the two dimensional ambiguity resolution simultaneously based on the 4 CPI data during one frame. While 2/2 criterion is adopted for the velocity ambiguity resolution and the range ambiguity resolution asynchronously by means of the multi-frame trajectory data. Based on the aforementioned analysis, the second generation mode of CVF is applied to the proposed method, in which the judgment criterion of the corresponding trajectory composition is designed as follows:

① If the maximum value of CVF and that of the N independent value functions satisfies equation (9), the CVF is considered to be formed by the noise measurement.

$$\frac{\max(\sum_i \mathrm{I}_{CPI\_i})}{N\left[\max(\mathrm{I}_{CPI\_1}, \mathrm{I}_{CPI\_2}, \cdots, \mathrm{I}_{CPI\_N})\right]} < (1-10^{-\delta/20}) \tag{9}$$

where the scale factor is set as $\delta = \min[20\log_{10}(\frac{\max(\sum_i \mathrm{I}_{CPI\_i})}{\eta_1}), 13]$. Herein, log stands for the logarithmic operation.

② If the maximum value of CVF and that of the N independent value functions satisfies equation (10), the CVF is considered to be formed by the mixed measurement, such as the noise, the multiple targets and the extended two-dimensional ambiguous data. Meanwhile, for different CPI data within each frame, we judge that there exist no coincidence between the real targets and their mixed measurement.

$$\left|\frac{\frac{\max(\sum_i \mathrm{I}_{CPI\_i})}{N} - \max(\mathrm{I}_{CPI\_1}, \mathrm{I}_{CPI\_2}, \cdots, \mathrm{I}_{CPI\_N})}{\max(\mathrm{I}_{CPI\_1}, \mathrm{I}_{CPI\_2}, \cdots, \mathrm{I}_{CPI\_N})}\right| \leq 10^{-\delta/20} \tag{10}$$

③ Analogous to the judgment criterion in ②, the CVF is considered to be formed by the mixed measurement in case

of equation (11) holds. The difference is that there exist several coincidences between the real targets and the mixed measurement among the multi-frame trajectory data.

$$\frac{\max(\sum_i \mathrm{I}_{CPI\_i})}{N\left[\max(\mathrm{I}_{CPI\_1}, \mathrm{I}_{CPI\_2}, \cdots, \mathrm{I}_{CPI\_N})\right]} > (1+10^{-\delta/20}) \tag{11}$$

Based on the above judgment criterion, for case ①, the adaptive threshold T_1 is equivalent to the CFAR threshold η_1, which is mainly used to eliminate the false alarm trajectories caused by noises.

In heterogeneous environment, the probability density function of the amplitude detectable quantity is given by [18]

$$f(x) = \frac{\gamma(\gamma-1)^{\gamma}}{(\gamma-1+x)^{\gamma+1}} \tag{12}$$

where $\gamma = (2m_2-2)/(m_2-2)$ denotes the heterogeneity degree of the observation scene. m_2 is the second-order statistics of the amplitude detectable quantity. Let the false alarm probability be P_{fa}, the CFAR threshold can be represented as

$$\eta_1 = \frac{\gamma-1}{\left(P_{fa}\right)^{1/\gamma}} + 1 - \gamma \tag{13}$$

Considering that the first level threshold is to eliminate the false alarm trajectories which possess relatively low amplitude for the CVFs. Also, to reduce the undetected probability of the real targets, a high false alarm probability is allowed. Therefore, P_{fa} is set to 10^{-3} in this section.

For case ② and case ③, the adaptive threshold T_1 is set to $\eta_1 + (\max(\sum_i \mathrm{I}_{CPI\_i}) - \eta_1)(1 - \frac{\eta_1}{\max(\sum_i \mathrm{I}_{CPI\_i})})$. It can be seen that T_1 is proportional to the difference between the maximum value of CVF and the CFAR threshold, which not only ensures the reliable target detection, but also reduces the false alarm trajectory number, including the trajectories composed of the noise measurement and those composed of the mixed measurement.

In conclusion, the first level threshold can be expressed as

$$T_1 = \begin{cases} \eta_1, & situation① \\ \eta_1 + (\max(\sum_i \mathrm{I}_{CPI\_i}) - \eta_1)(1 - \dfrac{\eta_1}{\max(\sum_i \mathrm{I}_{CPI\_i})}), & \\ & situation② \\ \eta_1 + (\max(\sum_i \mathrm{I}_{CPI\_i}) - \eta_1)(1 - \dfrac{\eta_1}{\max(\sum_i \mathrm{I}_{CPI\_i})}), & \\ & situation③ \end{cases} \tag{14}$$

Evidently, T_1 can be simplified as

$$T_1 = \begin{cases} \eta_1, & situation① \\ \max(\sum_i \mathrm{I}_{CPI\_i}) - \eta_1 + \dfrac{\eta_1^2}{\max(\sum_i \mathrm{I}_{CPI\_i})}, & \\ & situation, ③ \end{cases} \tag{15}$$

C. SECOND LEVEL THRESHOLD SETTING METHOD BASED ON TRAJECTORY CHARACTERISTICS

Compared with real targets, the locations of the false alarm points present a randomness in the inter-frame correlation gate, hence the distribution characteristics between the real target trajectories and the false alarm trajectories are significantly different. In this section, based on the first level adaptive threshold, the remaining false alarm trajectories are further eliminated according to the idea of polynomial regression. Firstly, the local polynomial fitting method is applied to the whole trajectories for each K_0 frame data set. Thus, solving the polynomial fitting coefficients is equivalent to calculating the minimum value in equation (16).

$$\min_{\boldsymbol{\beta}} \sum_{c=1}^{K-K_0+1} \sum_{k=c}^{c+K_0-1} \left(\sum_{i=0}^{Z} \beta_{c,i} (p_{x,k}^{m,n})^i - p_{y,k}^{m,n} \right)^2 \tag{16}$$

where $\boldsymbol{\beta} = \{\beta_{c,i}\}, c = 1, 2, \cdots, K-K_0+1, i = 0, 1, \cdots, Z$.

For the local trajectories started at the cth frame, the polynomial fitting coefficients $\beta = \left(\beta_{c,0}, \beta_{c,1}, \cdots, \beta_{c,Z}\right)^T$ can be obtained based on the least square method [19], as presented below.

$$\begin{pmatrix} 1 & p_{x,c}^{m,n} & (p_{x,c}^{m,n})^2 & \cdots & (p_{x,c}^{m,n})^Z \\ 1 & p_{x,c+1}^{m,n} & (p_{x,c+1}^{m,n})^2 & \cdots & (p_{x,c+1}^{m,n})^Z \\ \vdots & \vdots & & & \vdots \\ 1 & p_{x,c+K_0-1}^{m,n} & (p_{x,c+K_0-1}^{m,n})^2 & \cdots & (p_{x,c+K_0-1}^{m,n})^Z \end{pmatrix} \times \begin{pmatrix} \beta_{c,0} \\ \beta_{c,1} \\ \vdots \\ \beta_{c,Z} \end{pmatrix} = \begin{pmatrix} p_{y,c}^{m,n} \\ p_{y,c+1}^{m,n} \\ \vdots \\ p_{y,c+K_0-1}^{m,n} \end{pmatrix} \tag{17}$$

In equation (17), the least square solution is represented as $\beta = \mathrm{A}^{+}b$, where A is the coefficient matrix, which satisfies $\mathrm{A}^{+} = \left(\mathrm{A}^{\mathrm{T}}\mathrm{A}\right)^{-1}\mathrm{A}^{\mathrm{T}}$. The superscripts $(\cdot)^{+}$ and $(\cdot)^{\mathrm{T}}$ denote the generalized inverse operation and the transpose operation, respectively. b is a column vector, namely, $b = \left(p_{y,c}^{m,n}, p_{y,c+1}^{m,n}, \cdots, p_{y,c+K_0-1}^{m,n}\right)^{\mathrm{T}}$. Owing to the smooth trajectory characteristics of TS targets, Z is set to 2, which meet the polynomial fitting requirement of local trajectories. The polynomial fitting vector is given by

$$\beta = \left(\mathrm{A}^{\mathrm{T}}\mathrm{A}\right)^{-1}\mathrm{A}^{\mathrm{T}}\mathrm{b} \tag{18}$$

It can be seen that the local trajectory characteristics are fully exploited based on the above method by dividing the trajectory into K segments. Then, the global trajectory characteristics can be extracted by employing the global polynomial coefficient variance statistic, which is defined as

$$\Psi(\boldsymbol{\beta}) = \sum_{i=0}^{Z} \left[Var_{c=1}^{K-K_0+1}(\beta_{c,i}) \right] \tag{19}$$

where $\Psi(\boldsymbol{\beta})$ reflects the similarity of trajectory segments in the whole trajectory.

Thus, the false alarm trajectory elimination criterion is described as follows:

If $\Psi(\boldsymbol{\beta}) < \eta\frac{(Z+1)A_r}{SNR}$, then the candidate trajectory is regarded as the real target trajectory. Otherwise, it is determined as the false alarm trajectory. Here, the elastic coefficient η is set to 0.2, SNR represents the signal-to-noise ratio, A_r is the resolution cell, which is related to the radar system parameters.

D. TWO-STEP THRESHOLDS DP-TBD ALGORITHM

In order to improve the detection performance of TS targets, the two-step thresholds DP-TBD algorithm is proposed in this section, where the two-dimensional ambiguity resolution, the TS-target detection and the false alarm trajectory suppression problems are solved from the perspectives of the transmitting pulse sequence design, the CVF-based first level threshold setting strategy and the trajectory-based second level threshold setting strategy. Compared with Li method [14] and Zhu method [17], the TT pulse sequence is adopted in the proposed method to alleviate the target SNR loss caused by the range ambiguity and the spatial filling time. Moreover, the judgment criterion of the first level threshold setting procedure is given to adjust the threshold adaptively for different types of trajectories. That is, the false alarm trajectories are eliminated based on the composition of CVF. Finally, the false alarm trajectory number can be further reduced in the second level threshold setting procedure by utilizing the trajectory distribution characteristic difference between the local trajectory and the global trajectory. The main steps of the two-step thresholds DP-TBD algorithm are given below.

Step 1 Design of the transmitting pulse sequence.

Generating K frame echo data according to the TT pulse sequence.

Step 2 Construction of the extended ambiguous measurement.

Combined with the two-dimensional ambiguous number related to different CPIs, the extended ambiguous range-velocity measurement can be obtained. On this basis, the trajectory backtracking process is performed to get the corresponding value function and the candidate trajectory set.

Step 3 Generation of CVF.

Compared with the intra-frame 2/4 criterion [17], the multi-frame 2/2 criterion is adopted in the proposed method to resolve the two-dimensional ambiguity, where the cumulative SNR is applied to the trajectory ambiguity resolution process, and thus to promote the success probability of two-dimensional ambiguity resolution. Based on the TT ambiguity resolution strategy, the candidate target trajectory set and the corresponding CVFs can be achieved by summing the overlapped trajectory measurements related to different CPIs. Here, the ambiguity resolution performance of different algorithms will be detailedly analyzed in section IV.

Step 4 Setting the first level threshold.

For each backtracking trajectory, the judgment criterion of the trajectory composition is designed based on the relationship between its CVF and the corresponding N value functions, as a result, the candidate target trajectory set can be obtained by employing the first level threshold.

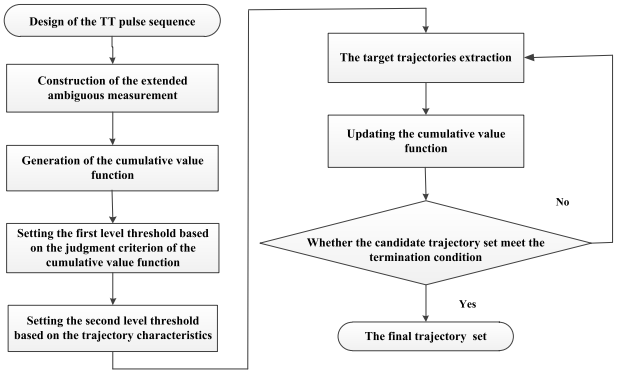

FIGURE 3. Flow chart of the two-step thresholds DP-TBD algorithm.

Step 5 Setting the second level threshold.

The local trajectory characteristics and the global trajectory characteristics are combined to form the polynomial coefficient variance statistics, then the candidate target trajectory set is updated by means of the second level threshold.

Step 6 Extraction of the target trajectory set.

Seeking for the maximum value of CVF in the candidate trajectory set, which is considered belonging to a real target trajectory. Meanwhile, those trajectories coincided with the existing target trajectory for more than $L(L = K/3)$ frame are eliminated [12].

Step 7 CVF update.

Suppose that the extended ambiguous position measurement can be expressed as $\{\boldsymbol{P_x}, \boldsymbol{P}_y\}$. $V_{sum}\{\boldsymbol{P_x}, \boldsymbol{P}_y\}$ and $V_{CPI\_n}\{\boldsymbol{P_x}, \boldsymbol{P}_y\}$ stand for the corresponding trajectory backtracking amplitude of CVF and that of the value function with regard to CPI_n, where the update criteria of $V_{sum}\{\boldsymbol{P_x}, \boldsymbol{P}_y\}$ is represented as

$$V_{sum}\{\boldsymbol{P_x}, \boldsymbol{P}_y\} = V_{sum}\{\boldsymbol{P_x}, \boldsymbol{P}_y\} - \max_n V_{CPI\_n}\{\boldsymbol{P_x}, \boldsymbol{P}_y\} \quad (20)$$

Based on the above analysis, the updated CVF can be generated according to equation (20).

Step 8 Judging whether the candidate trajectory set meets the termination condition.

If the maximum value of the updated CVF and that of the N independent value functions conform to equation (21), stop iteration and output the target trajectory set; Otherwise, turn to step 6 and repeat the searching process for the new target trajectories.

$$\max(\sum_i \mathrm{I}_{CPI\_i}) < \frac{N\left[\max(\mathrm{I}_{CPI\_1}, \mathrm{I}_{CPI\_2}, \cdots, \mathrm{I}_{CPI\_N})\right]}{2} \quad (21)$$

FIGURE. 3 demonstrates the flow chart of the two-step thresholds DP-TBD algorithm.

IV. EXPERIMENTAL RESULTS

Considering that there is no published real measured data for TS targets, without loss of generality, the simulation results of

multi-target echoes are generated in serious two-dimensional ambiguity and low SNR environment, and hence the performance of the proposed algorithm is evaluated comprehensively from three aspects, i.e. ambiguity resolution, detection probability and the false alarm trajectory suppression ability.

A. TWO-DIMENSIONAL AMBIGUITY RESOLUTION PERFORMANCE ANALYSIS

Let K, $Time_f$ and P_{fa} be the observation frame number, the spatial filling time and the false alarm probability, respectively. It is assumed that the SNRs are constant for the four CPIs in each frame. P_1 represents the detection probability in one CPI, while P_2 stands for that after taking the spatial filling problem into account. P_3 indicates the trajectory detection probability with regard to one PRF. Obviously, P_2 and P_3 can be calculated according to P_1, K, $Time_f$ and P_{fa} [20]. Here, the spatial filling time $Time_f$ and P_{fa} are set as CPI/4 and 10^{-3}, where $Time_f$ should be greater than the time delay caused by range ambiguity. In fact, $Time_f$ may be higher as a result of the wide coverage characteristic for surveillance radar.

The success ambiguity resolution probability of the above two ways to generate the CVF are analyzed quantitatively in this section, in which the first generation mode and the second generation mode are adopted in TT method and Zhu method separately. That is, the means of the trajectory ambiguity resolution and that of the intra-frame ambiguity resolution are applied to these two approaches in turn. For TT method, the success probability of the velocity ambiguity resolution and that of the range ambiguity resolution based on the multi-frame trajectory data can be expressed by $(1-(1-P_3^2)^2)$ and $(1-(1-P_3)^2)^2$, and thus the success probability of two-dimensional ambiguity resolution is given by $(1-(1-P_3^2)^2)\times(1-(1-P_3)^2)^2$. For Zhu method, the two-dimensional ambiguity resolution is accomplished synchronously using multiple sets of PRF data. However, considerable spatial filling time should be reserved between adjacent $PRFs$ to separate different CPI data, and the corresponding success probability of two-dimensional ambiguity resolution is represented as $\left(1-(1-P_2)^4-4P_2(1-P_2)^3\right)^K$. With the increase of the observation frame number, the success probability of two-dimensional ambiguity resolution related to the second CVF can be improved as a result of its multi-frame detection strategy. FIGURE. 4 shows the success probability curves of two-dimensional ambiguity resolution using different methods, where P_1 is selected as the horizontal coordinate value. One can see that the success ambiguity resolution probability of TT method possesses significant performance improvement than that of Zhu method, which is consistent with the theoretical analysis in section III.

B. DETECTION PERFORMANCE ANALYSIS

Assume that the observation scene is composed of 22500 units (150 range units $\times$ 150 velocity units), in which 6 targets move independently with uniform speeds. Let the initial motion state of the mth target be $[p_0^m, v_0^m]^T$,where

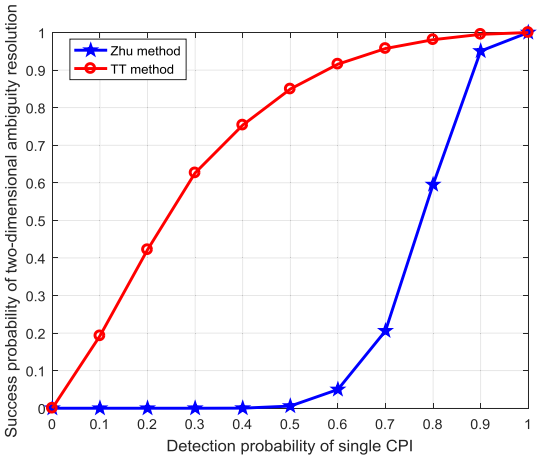

FIGURE 4. Success probability of two-dimensional ambiguity resolution.

p_0^m and v_0^m stand for the measured range and the measured velocity, $m = 1, \cdots, 6$. Here, the initial states of these 6 targets are set as [10,30], [54, 60], [70, 105], [80, 65], [85, 35] and [100, 100]. For each CPI, the relationship between the SNR and the target amplitude satisfies SNR $= 10\lg(A^2/\sigma^2)$, where A and σ indicate the target amplitude and standard deviation of noise, respectively.

FIGURE. 5(a) and FIGURE. 5(b) demonstrate the energy accumulation diagrams with respect to no ambiguity case and two-dimensional ambiguity case, where the single frame SNR of each target is 8dB, both the range ambiguity number and the velocity ambiguity number are set to 8, the total accumulative frame number K is given by 8. Obviously, there are many false alarm peaks in the observation scene after multi-frame energy accumulation for two-dimensional ambiguity case. Meanwhile, there are no evident peaks located in the real target position. As a result, traditional CFAR detection methods will inevitably lead to the missing detection of real targets as well as the increase of false alarm target number.

In order to evaluate the detection performance in serious two-dimensional ambiguity and low SNR environment, the detection probability curves versus SNR based on Li method, Zhu method and the proposed method are compared in FIGURE. 6, in which Monte Carlo simulation times is selected as 500, the range-velocity ambiguity number related to the two $PRFs$ in TT method are set to $(7, 5)$, $(11, 4)$, while the range-velocity ambiguity number related to the four $PRFs$ in Li method and Zhu method are set to $(5, 6)$, $(7, 5)$, $(11, 4)$, $(13, 2)$ in turn. Here, successful detection of a candidate target meets the condition that the amplitude of CVF exceeds the adaptive threshold, and its position deviation from the real target in range-Doppler domain is less than one resolution within each frame.

Compared with Li method and Zhu method, the proposed algorithm presents excellent detection performance for all the 6 targets. Among these methods, the missing detection problem can be avoided by means of Li method as a result of employing one-step prediction strategy in the

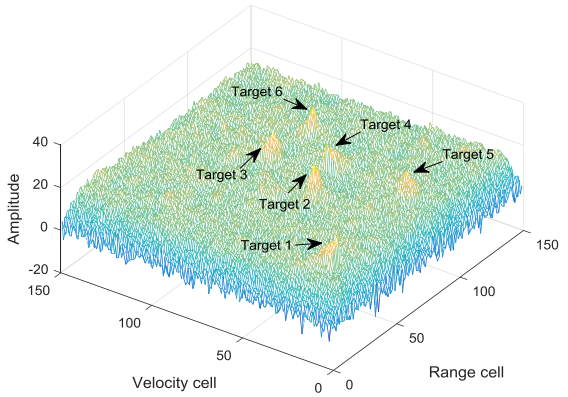

(a) The accumulated energy with no ambiguity

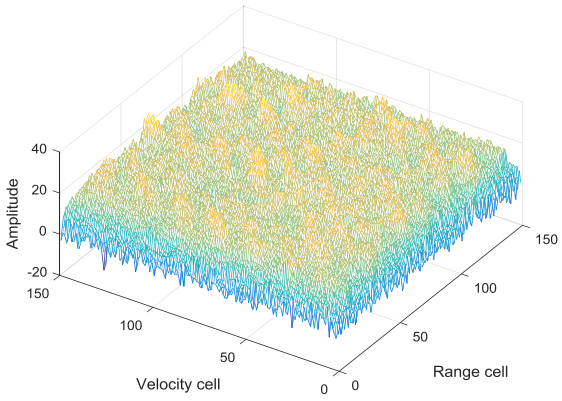

(b) The accumulated energy with two-dimensional ambiguity

FIGURE 5. Energy accumulation diagrams.

update process of CVF. However, the renewal process of the extended ambiguous range-velocity measurement is not taken into consideration, which leads to the increase of the first level adaptive threshold as well as the deterioration of multi-target detection performance. For Zhu method, the ambiguity-resolved data is achieved based on intra-frame data rather than inter-frame data, in which the advantage of 4 *PRFs* combination processing is discarded, and thus result in the accumulated energy loss, especially for low SNR target. Meanwhile, the number of false alarm trajectories is greatly increased in the trajectory backtracking process because a large number of ghost targets are formed when conducting the intra-frame ambiguity resolution procedure. Also, this method could only eliminate part of the ghost targets within each frame, but not the false alarm trajectories generated from multi-frame association, which is not suitable for joint TBD processing. For the proposed method, the TT pulse sequence is adopted to reduce the range ambiguity number and shorten the spatial filling time between adjacent *PRFs*. Moreover, the generation of CVF is accomplished before the trajectory ambiguity resolution process. In this way, the original CPI data within each frame can be retained to avoid the accumulated energy loss. Further, we take target 5, which has the worst detection probability among the 6 targets, as an example to verify the reliability of the aforementioned theoretical analysis. One can see that the detection probability curve of the proposed method increases faster than those of other methods, which shows obvious superiority under the condition of low SNR environment (SNR<8dB), as shown in FIGURE. 6.

C. FALSE ALARM PERFORMANCE ANALYSIS

The multi-target detection performance in serious two-dimensional ambiguity and low SNR environment has been demonstrated in the last section. Here, different methods are employed to handle the candidate trajectory set and thus to evaluate their false alarm performance, where the corresponding CVFs are considered to be formed by three types of false alarm trajectories, i.e., the noise trajectory, the extended ambiguous measurement trajectory and those composed of the mixed measurement. Therefore, the false alarm trajectory suppression methods should meet the inhibition ability for the above mentioned false alarm trajectories. In order to compare the false alarm trajectory suppression ability of different methods intuitively, two-dimensional cartesian coordinate system is adopted to reveal the trajectory distribution characteristics. According to equation (11), the extended ambiguous measurement positions of the k th frame, the n th CPI and the m th target can be expressed as

$$\begin{cases} \tilde{p}_{x,k}^{m,n} = \tilde{r}_k^{m,n} \cos(\theta_k^{m,n}) \\ \tilde{p}_{y,k}^{m,n} = \tilde{r}_k^{m,n} \sin(\theta_k^{m,n}) \end{cases} \tag{22}$$

Figure 7 shows the candidate target trajectories using different detection methods, where the red curves represent the real target trajectories, and the blue curves indicate the candidate trajectories, SNR is set to 6dB. In Figure 7(a), the extended ambiguous measurement is neglected in the CVF update process with regard to Li method, which leads to a large number of false alarm trajectories in the candidate trajectory set. In Figure 7(b), ambiguity matrix completion and elimination strategy is adopted to form the CVF based on Zhu method, and this method can only suppress the ghost targets generated within a single frame, but not the false alarm trajectories formed within multiple frames, so it is not suitable for multi-frame joint detection. In contrast, the false alarm trajectory number based on the proposed method reduces significantly by applying the transmitting pulse sequence design method combined with the CVF-based first level threshold setting strategy, as presented in Figure 7(c). This is due to the range ambiguity number decreases substantially by employing the transmitting TT method, and hence the adaptive detection threshold can be obtained through mining the trajectory composition of CVF in the first level threshold setting process, in which the false alarm trajectories can be eliminated more efficiently under the premise of robust multi-target detection.

Figure 8 contrasts the trajectory processing results with different algorithms. In Figure 8(a), the trajectory update technique based on one-step prediction strategy, proposed

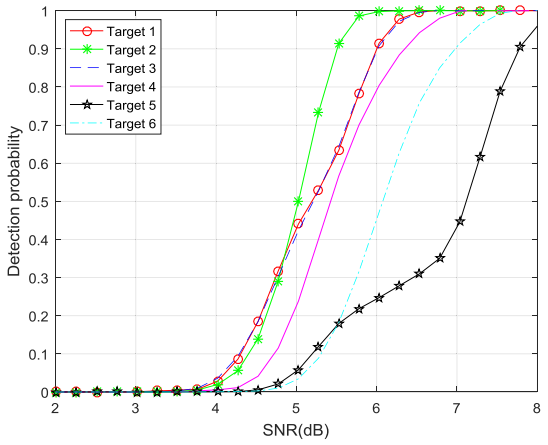

(a)Detection probability using Li method

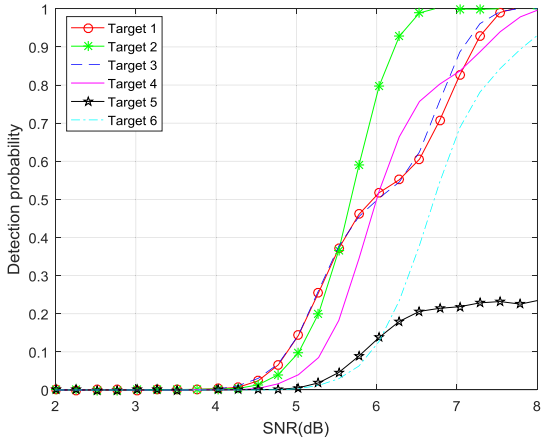

(b)Detection probability using Zhu method

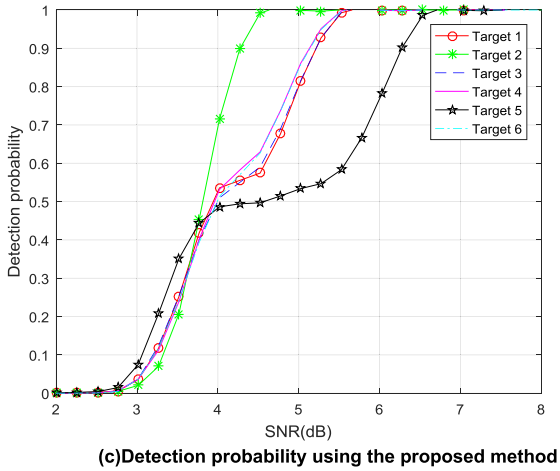

(c)Detection probability using the proposed method

FIGURE 6. Detection probability using different methods.

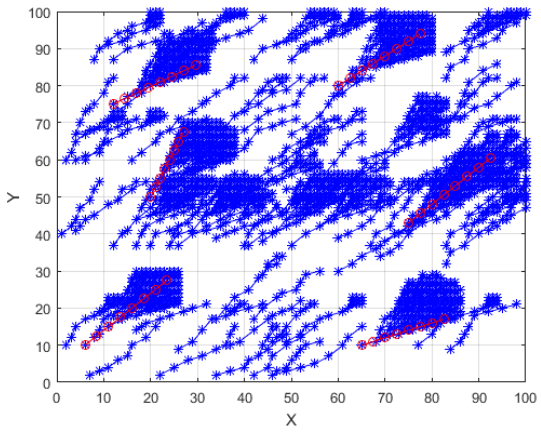

(a) The candidate trajectories using Li method

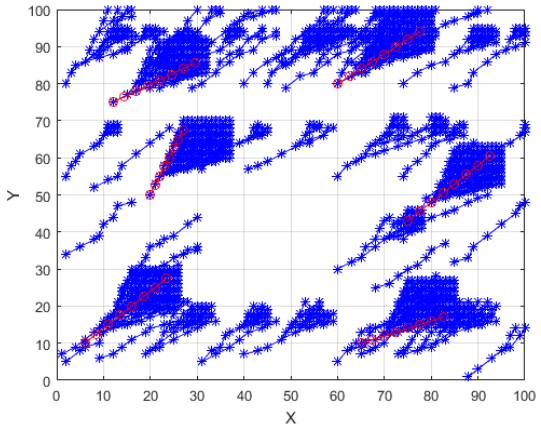

(b) The candidate trajectories using Zhu method

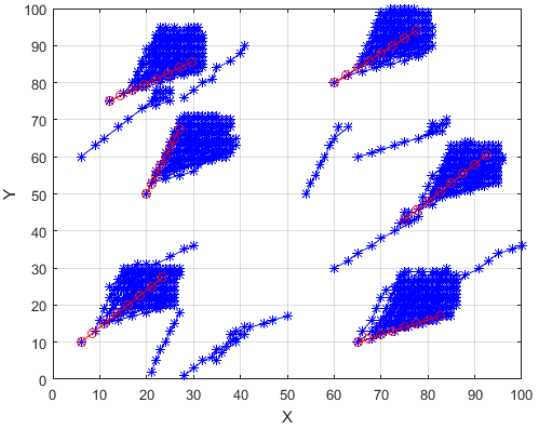

(c) The candidate trajectories using the proposed method

FIGURE 7. The candidate trajectories using different methods.

in Li method, could reduce the target energy loss caused by adjacent or intersecting jammings, but cannot effectively deal with the false alarm trajectories caused by the extended ambiguous measurement. Figure 8(b) demonstrates the extracted trajectories using the joint strategy, i.e. trajectory overlapping, direction histogram statistics and Zhu method, which is simply applicable for suppressing the noise trajectories as well as those which share several frame data with the real target trajectory. Therefore, there still exists a certain number of false alarm trajectories after

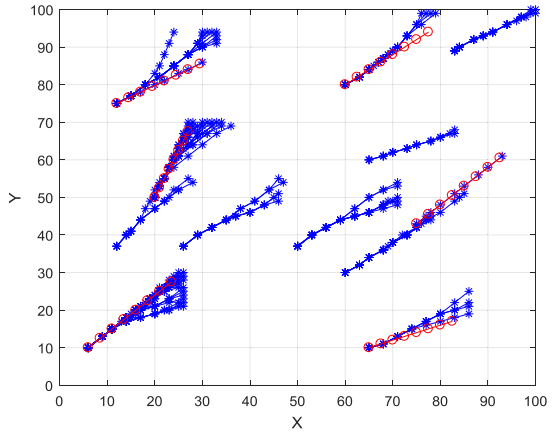

(a) The extracted trajectories using Li method

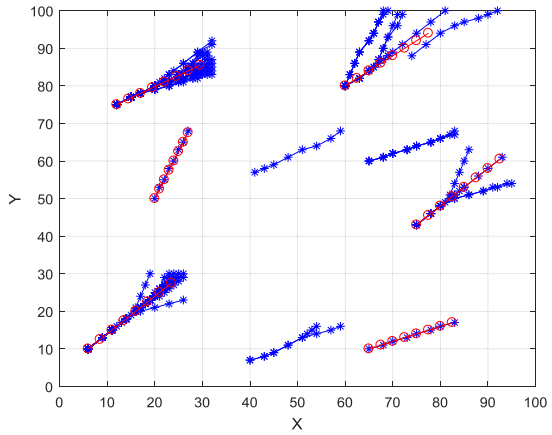

(b)The extracted trajectories using the joint strategy, i.e. trajectory overlapping, direction histogram statistics [21] and Zhu method

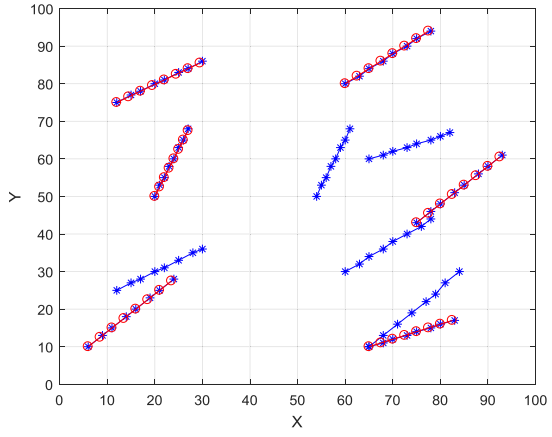

(c) The extracted trajectories using the proposed method

FIGURE 8. The trajectory processing results using different algorithms.

trajectory processing. For the proposed method, the second level threshold related to the local trajectory characteristics and the global trajectory characteristics is derived to eliminate different types of false alarm trajectories, as shown in Figure 8(c). One can see that only a few false alarm trajectories with high similarity to the real target trajectory are included among the extracted trajectories. Besides, target 6 is not contained in the extracted trajectories in terms of Figure 8(a) and Figure 8(b). That is, target 6 is not successfully detected by means of Li method and Zhu method on condition that SNR $=$ 6dB, which is consistent with the numerical results presented in Figure 6.

V. CONCLUSION

A two-step thresholds TBD algorithm based on dynamic programming is proposed to solve TS target detection problem in low SNR environment, where the transmitting pulse sequence, the adaptive amplitude threshold of CVF and the global polynomial coefficient variance statistic are designed sequentially. On one hand, the TT pulse sequence is adopted in the transmitting pulse sequence, which is conductive to the multi-target detection and the two-dimensional ambiguity resolution. On the other hand, different types of false alarm trajectories are effectively eliminated through judging the trajectory composition of CVF and exploiting the relationship among the multi-frame trajectory data. Experimental results indicate that the proposed algorithm improves both the success probability of ambiguity resolution and the multi-target detection performance. However, the final target trajectory set still contains a few false alarm trajectories, which possess extremely similar trajectory characteristics to that of the real target. Therefore, our future work will concentrate on extracting other depth characteristics based on our existing research to obtain better TS target detection performance.

ACKNOWLEDGMENT

The authors would like to thank the associate editor and anonymous reviewers for their insightful comments and suggestions. *(Yu Li, Caipin Li, and Min Tian contributed equally to this work.)*

REFERENCES

[1] R. Jin, W. Zhou, J. Yin, and J. Yang, "CFAR line detector for polarimetric SAR images using Wilks' test statistic," *IEEE Geosci. Remote Sens. Lett.*, vol. 13, no. 5, pp. 711–715, May 2016.

[2] Y. B. Rui, Z. H. Wei, and N. Khoasang, "A multi strategy CFAR detector under non-uniform background," *J. Nanjing Univ. Sci. Technol.*, vol. 40, no. 2, pp. 199–203, 2016.

[3] W. Yi, L. Kong, and J. Yang, "Thresholding process based dynamic programming track-before-detect algorithm," *IEICE Trans. Commun.*, vol. 96, no. 1, pp. 291–300, 2013.

[4] X. Y. Cao, Z. J. Zhang, and J. J. Xiang, "Detection and tracking of radar dim targets based on improved dynamic programming," *Mod. Defence Technol.*, vol. 41, no. 4, pp. 149–154, 2016.

[5] L. A. Johnston and V. Krishnamurthy, "Performance analysis of a dynamic programming track before detect algorithm," *IEEE Trans. Aerosp. Electron. Syst.*, vol. 38, no. 1, pp. 228–242, Jan. 2002.

[6] W. Yi, L. Kong, J. Yang, and X. Deng, "A tracking approach based on dynamic programming Track-Before-Detect," in *Proc. IEEE Radar Conf.*, May 2009, pp. 1–4.

[7] S. C. Tan, G. H. Wang, N. Wang, and H. B. Yu, "Joint range ambiguity resolving and multiple maneuvering targets tracking in clutter via MMPHDF-DA," *Sci. China Inf. Sci.*, vol. 8, p. 82311, Feb. 2014.

[8] L. Li, G. Wang, X. Zhang, and H. Yu, "A TBD algorithm for near space hypersonic target under the condition of range ambiguity," in *Proc. 2nd IEEE Int. Conf. Comput. Commun. (ICCC)*, Oct. 2016, pp. 2840–2844.

[9] G. Wang, S. Tan, C. Guan, N. Wang, and Z. Liu, "Multiple model particle filter track-before-detect for range ambiguous radar," *Chin. J. Aeronaut.*, vol. 26, no. 6, pp. 1477–1487, Dec. 2013.
[10] H. B. Yu, G. H. Wang, Q. Cao, and N. Wang, "A novel approach for detecting and tracking weak targets in high-PRF radar," *J. Electron. Inf. Technol.*, vol. 37, no. 5, pp. 1097–1103, 2015.
[11] X. Bi, J. Du, Q. Zhang, and W. Wang, "Improved multi-target radar TBD algorithm," *J. Syst. Eng. Electron.*, vol. 26, no. 6, pp. 1229–1235, Dec. 2015.
[12] L. Yu, "Multi-objective GMTI-TBD technology based on dynamic programming," *Chin. J. Sci. Instrum.*, vol. 37, no. 2, pp. 356–364, 2016.
[13] R. Liu, W. G. Wang, and C. Y. Qiu, "Target identification method based on dynamic programming in pre detection tracking algorithm," *Fire Control Command Control*, vol. 36, no. 1, pp. 67–70, 2011.
[14] Y. Li, J. Zhu, and J. Zhang, "Two-step detection algorithm for fluctuating weak target based on dynamic programming," *J. Eng. Technol. (JET)*, vol. 10, no. 1, 2019.
[15] A. Clive, *Pulse Doppler Radar Principles, Technology, Application*. Beijing, China: Publishing House of Electronics Industry, 2015.
[16] D. C. Schleher, *MTI and Pulsed Doppler Radar With MATLAB*. Beijing, China: Publishing House of National Defense Industry, 2009.
[17] J. Zhu, Y. Li, C. Duan, W. Wang, C. Wen, and Y. Huang, "A range and velocity ambiguity resolution method based on ambiguity matrix completion and elimination with low SNR," in *Proc. IEEE Int. Conf. Signal, Inf. Data Process. (ICSIDP)*, Dec. 2019, pp. 1–6.
[18] M. Tian, Z. Yang, H. Xu, G. Liao, and W. Wang, "An enhanced approach based on energy loss for multichannel SAR-GMTI systems in heterogeneous environment," *Digit. Signal Process.*, vol. 78, pp. 393–403, Jul. 2018.
[19] K. Deckers and A. Bultheel, "Rational interpolation: I. least square convergence," *J. Math. Anal. Appl.*, vol. 395, no. 2, pp. 455–464, Nov. 2012.
[20] M. Skolnick, *Radar Handbook*. New York, NY, USA: McGraw-Hill, 2008.
[21] C. Duan, Y. Li, and W. W. Wang, "An intelligent sample selection method for space-time adaptive processing in heterogeneous environment," *IEEE Access*, vol. 7, pp. 30321–30330, 2019.

YU LI received the B.Sc. degree from Northwest University, in 2011, and the M.Sc. and Ph.D. degrees from the Xi'an Institute of Space Radio Technology, in 2014 and 2018, respectively. He is currently with the Xi'an Institute of Space Radio Technology. His main research interests include moving target detection and tracking and radar imaging.

CAIPIN LI received the B.Sc. degree from Air Force Engineering University, the M.Sc. degree from the Xi'an Institute of Space Radio Technology, and the Ph.D. degree from Northwest Polytechnic University. He is currently with the Xi'an Institute of Space Radio Technology. His main research interest includes high-orbit SAR imaging.

MIN TIAN received the M.Sc. and Ph.D. degrees from Xidian University. She is currently with the Xi'an Institute of Space Radio Technology. Her main research interest includes ground moving target indicator.

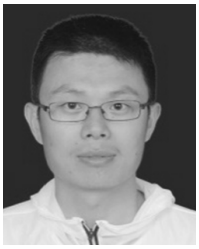

WEIWEI WANG received the B.Sc., M.Sc., and Ph.D. degrees from Xidian University, in 2005, 2008, and 2013, respectively. He is currently a Senior Engineer with the Xi'an Institute of Space Radio Technology. His main research interest includes ground moving target indicator.

CHONGDI DUAN received the B.S. degree from the Harbin Institute of Technology, in 1994, and the M.S. degree from the School of Electronic Engineering, Xidian University, in 2005. He is currently pursuing the Ph.D. degree with the School of Beijing Institute of Technology. He is also a Professor with the National Key Laboratory of Science and Technology on Space Microwave, Xi'an Institute of Space Radio Technology. His research interests include adaptive and array signal processing, high-speed real-time signal processors, and so on.

XUYAN WANG received the M.Sc. and Ph.D. degrees from Northwest Polytechnic University. She is currently a Senior Engineer with the Xi'an Institute of Space Radio Technology. Her main research interest includes SAR imaging.